JOURNAL OF BACTERIOLOGY, Feb. 1988, p. 669–675
0021-9193/88/020669-07$02.00/0

Vol. 170, No. 2

Immunological Characterization of Ice Nucleation Proteins from *Pseudomonas syringae*, *Pseudomonas fluorescens*, and *Erwinia herbicola*

CAROLINE A. DEININGER, GUNHILD M. MUELLER, AND PAUL K. WOLBER*

Advanced Genetic Sciences, Inc., 6701 San Pablo Avenue, Oakland, California 94608

Received 26 June 1987/Accepted 11 November 1987

Antibodies were raised against the InaW protein, the product of the ice nucleation gene of *Pseudomonas fluorescens* MS1650, after protein isolation from an *Escherichia coli* clone. On Western blots (immunoblots), these antibodies recognized InaW protein and InaZ protein (the ice nucleation gene product of *Pseudomonas syringae* S203), produced by both *E. coli* clones and the source organisms. The InaZ protein appeared in *P. syringae* S203 during stationary phase; its appearance was correlated with the appearance of the ice nucleation-active phenotype. In contrast, the InaW protein occurred at relatively constant levels throughout the growth phases of *P. fluorescens* MS1650; the ice nucleation activity was also constant. Western analyses of membrane preparations of *P. syringae* PS31 and *Erwinia herbicola* MS3000 with this antibody revealed proteins which were synthesized with development of the nucleating phenotype. In these species the presence or absence of the nucleating phenotype was controlled by manipulation of culture conditions. In all nucleation-positive cultures examined, cross-reacting low-molecular-weight bands were observed; these bands appeared to be products of proteolytic degradation of ice nucleation proteins. The proteolysis pattern of InaZ protein seen on Western blots showed a periodic pattern of fragment sizes, suggesting a highly repetitive site for protease action. A periodic primary structure is predicted by the DNA sequence of the *inaZ* gene.

The ability of some species of gram-negative bacteria from the genera *Pseudomonas* (1, 2, 21, 22), *Erwinia* (19), and *Xanthomonas* (23) to nucleate the crystallization of ice demonstrates a unique manipulation of the environment by bacteria. Such bacteria are the major nucleating agents found on the leaves and flowers of many plants (16, 17, 20) and initiate much of the damage done to crops by frost. The ice nucleation-active (Ina^+) phenotype may confer a selective advantage on bacteria which express it; whether this advantage exists has been the subject of speculation (17, 18). Thus, bacterial ice nuclei present a puzzle with important evolutionary, ecological, and economic implications.

The Ina^+ phenotype is imparted by one structural gene in various strains of *Pseudomonas syringae* (11, 23) and *P. fluorescens* (5). The genes from two *Pseudomonas* species have been sequenced and found to encode homologous proteins (11, 29); strains of *Escherichia coli* transformed with these genes exhibit the Ina^+ phenotype. Much of the amino acid sequence deduced from either gene is composed of interleaved repetitions of 8, 16, and 48 amino acids. These conserved, repetitive sequences suggest that the function of ice-nucleating proteins is the formation of an ice crystal template (29).

Bacterial ice nuclei may be localized in the outer membranes of the source organisms (17) and may be membrane-bound protein aggregates (A. G. Govindarajan and S. E. Lindow, Plant Phys. **75**:94, 1984; S. E. Lindow, Phytopathology **73**:809, 1983). Subcellular fractions have been enriched in ice nucleation activity by fractionation of bacterial membranes (17, 32) and by concentration of nuclei shed by *Erwinia herbicola* (24). Two ice nucleation proteins have been identified after overexpression in *E. coli* (5, 32). Finally, ice nuclei containing the product of the *inaZ* gene as their only protein component have been purified from transformed *E. coli* (32); these nuclei are active only at temperatures below −8°C.

The precise relationship between ice nucleation proteins and the Ina^+ phenotype remains unclear. Many models for the role of ice nucleation proteins have been proposed (3, 14, 29). Such models are premature when two basic questions remain unanswered. Are ice nucleation proteins detectable in the organisms which are sources of ice nucleation genes, and are these proteins present only if the Ina^+ phenotype is present? This work reports results obtained with a polyclonal antibody raised against one ice nucleation protein. This antibody was used to answer the questions posed above, to identify two previously uncharacterized ice nucleation proteins, and to discover phenomena which indicate that the secondary structure of at least one nucleation protein is periodic.

MATERIALS AND METHODS

Chemicals, bacterial strains, and culture conditions. All chemicals were reagent grade, purchased from Sigma Chemical Co. unless otherwise noted. Bacto-peptone, yeast extract, tryptone, nutrient broth, and agar were from Difco Laboratories (Detroit, Mich.). Strains used in these experiments are listed in Table 1. Cultures were grown in either Luria broth (LB) (32) or nutrient agar-glycerol (NAG) (20). Solid media were prepared by adding 15 g of agar per liter of broth.

Inoculation and harvest procedures. Cells from frozen (−80°C) stocks in 20% dimethyl sulfoxide were streaked on NAG plates and grown at 24°C for 48 h. Inoculum derived from a single colony was spread on a fresh NAG plate; after overnight incubation at 24°C, cells were harvested from plates by adding 5 ml of sterile H_2O and loosening the cells with a spreader. This cell slurry was diluted (sterile H_2O) to an optical density at 600 nm of 0.1. Multiple NAG plates were inoculated by spreading 0.10 ml of this suspension and

* Corresponding author.

TABLE 1. Bacterial strains used in this study

Species and strain	Relevant genotype or phenotype	Source or reference
Pseudomonas syringae		
S203	Wild type, Ina$^+$	30
RGP36	S203 Δ*inaZ99* Ina$^-$	30
PS31	Wild type, Ina$^+$	2
Pseudomonas fluorescens		
MS1650	Wild type, Ina$^+$	30
GJP17B	MS1650 Δ*inaW1* Ina$^-$	30
Erwinia herbicola		
MS3000	Wild type, Ina$^+$	This laboratory
Erwinia carotovora		
Ecc301	Wild type, Ina$^-$	This laboratory
Escherichia coli K-12		
JC10291	Ina$^-$, *recA*	31
LC41	JC10291(pLVC41), Ina$^+$	5
MS10	JC10291(pMWS10), Ina$^+$	32
CD3	JC10291(pUC9), Ina$^-$	28
CD7	JC10291(pACYC184), Ina$^-$	4

then incubated at 24°C until harvest. Cells with poor ice nucleation activity were obtained from liquid cultures grown for 24 to 48 h at room temperature in LB with shaking; *E. coli* were cultured in LB (32).

Measurement of ice nucleus and bacterial populations. Ice nucleation spectra were measured by the drop-freezing method of Vali (27). Cell concentrations were determined by counting cells on a hemacytometer or by counting colonies from a serial dilution plating. Cell numbers measured by the two methods differed by less than 10%. Concentrations determined from plate counts (average of three or four plates) were used to calculate the number of nuclei per CFU for ice nucleation spectra.

Nucleating preparations. Early in this work, total membrane fractions were isolated by the method of Ito et al. (13). Later, a rapid method of obtaining a fraction containing all of the cellular ice nuclei and ice nucleation protein was developed. A suspension of 10^{10} cells in 1 ml of 10 mM NaP_i buffer (pH 7.0) was brought to 1 mM *o*-phenanthroline, 1 mg of lysozyme per ml, 10 mM EDTA, and 40 mM octylthio-β-D-glucopyranoside (OSG; Calbiochem). After 15 min of incubation on ice, membrane material was aggregated by addition of $MgCl_2$ (50 mM), and DNA was degraded by addition of DNase (0.1 mg/ml; Calbiochem). After a second 15-min incubation on ice, the membrane material was pelleted in a microfuge (30 min, 4°C). The supernatant was removed, and the pellet was suspended in ice-cold 10 mM $MgCl_2$ (pH 7.0). Examination of all fractions produced by this method showed that >99% of the ice nuclei and nearly all of the detectable ice nucleation protein were concentrated in the membrane pellet (data not shown). Unless otherwise stated, nucleating samples for this work were prepared by this method.

Protein concentration determination and PAGE. Protein concentrations were determined by the bicinchoninic acid method (25; Pierce Chemical Co.). Membranes were solubilized by boiling for 15 min in 1% (wt/vol) sodium dodecyl sulfate (SDS) and then diluted to 0.1% SDS. Samples of unknowns and blanks were assayed in 0.1% SDS. One-dimensional SDS-polyacrylamide gel electrophoresis (SDS-PAGE) was performed as described by Laemmli (15). Linear gradient gels (4 to 15% polyacrylamide) with 3% stacking gels were used in most experiments. The sample solubilization buffer included 8 M urea.

Preparation of anti-InaW protein antibody. Samples of the InaW protein heterologously expressed by *E. coli* LC41 were prepared by electroelution (12) from a preparative SDS-polyacrylamide gel (first immunization), by OSG extraction (32) of total bacterial membranes (first booster), or by column purification (all subsequent boosters [32]). All immunizations were done with pure InaW protein, as judged by SDS-PAGE. Purified protein samples were dialyzed against 1 liter of sterile 50 mM $(NH_4)HCO_3$ buffer (pH 7.0) at 4°C, concentrated in a vacuum-centrifuge (Savant), brought to the final volume with sterile phosphate-buffered saline (PBS; 10 mM NaP_i, 150 mM NaCl, pH 7.0), and stored frozen at −20°C. Polyclonal antisera were produced by Berkeley Antibody Co., Inc. (Richmond, Calif.). An immunoglobulin G (IgG)-rich fraction of the antiserum was obtained by ammonium sulfate precipitation (7).

Anti-*E. coli* antibodies present in the antiserum were preabsorbed from the immunoglobulin fraction by a modification of the method of Young and Davis (33), with Ina$^-$ *E. coli* membranes (13). Membranes were solubilized by boiling in 1% (wt/vol) SDS, diluted 1:20 with PBS, and bound to nitrocellulose filters. The filters were blocked with 3% gelatin in PBS, washed with PBS, and incubated with antiserum for 1 h at room temperature.

Electrophoretic blotting and Western (immunoblot) analysis. After separation by SDS-PAGE, protein bands were transferred to nitrocellulose filters (0.2 μm pores; Schleicher & Schuell) by a modification of standard methods (26). Prestained molecular size standards (Bethesda Research Laboratories) were used to mark molecular sizes on blots. Transverse electrophoresis was performed in a buffer containing 192 mM glycine, 25 mM Tris base, and 5% (vol/vol) methanol, in a high-field apparatus (Bio-Rad Laboratories) at 100 V for 2 h. Prior to transblotting, gels were soaked for 5 min in the same buffer plus 0.1% (wt/vol) SDS.

The transblotted nitrocellulose filters were probed with anti-InaW polyclonal antibody. Immunochemical staining of the labeled band(s) was performed with an avidin-biotin-horseradish peroxidase (ABC) system designed for use with rabbit antisera (Vectastain; Vector Laboratories, Burlingame, Calif.) as specified by the manufacturer. Labeled bands were visualized by the color-producing reaction of horseradish peroxidase with 4-chloronaphthol (Bio-Rad) as the substrate.

Degradation time course. The nucleating fraction of stationary-phase *P. syringae* S203 was prepared with the omission of *o*-phenanthroline. Five samples of 50 μl each were incubated at 20°C for various amounts of time. Portions were tested for ice nucleation activity and prepared for SDS-PAGE after 0, 0.5, 1, 5, and 19 h at 20°C.

RESULTS

Demonstration of specificity of the antibodies. Preparations from Ina$^+$ and Ina$^-$ *E. coli* cells were solubilized and separated by SDS-PAGE. The separated proteins were then analyzed by Western blotting, using the immunoglobulin fraction purified from the rabbit antiserum raised against InaW protein (anti-InaW) as the probe. The results of this analysis is shown in Fig. 1A. When used to probe proteins from the Ina$^+$ *E. coli* strain LC41 (Fig. 1A, lane 1), anti-InaW reacted strongly with a band at the known migration position of the InaW protein (5). This was expected, since

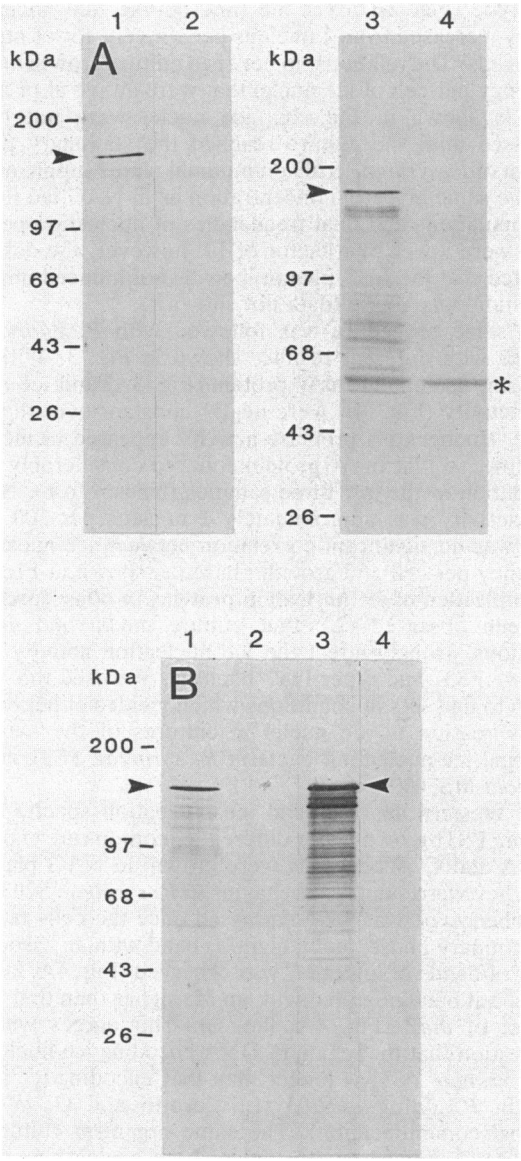

FIG. 1. Western analysis of proteins from Ina$^+$ and Ina$^-$ bacterial strains. (A) Lane 1, LC41 (*E. coli* carrying the *inaW* gene); lane 2, CD7 [*E. coli* JC10291(pACYC184), Ina$^-$ control]; lane 3, *P. fluorescens* MS1650 (the naturally occurring Ina$^+$ source organism of the *inaW* gene); lane 4, *P. fluorescens* GJP17B (the Ina$^-$ deletion mutant of MS1650). The band seen at 60 kDa in lane 4 (*) was due to nonspecific binding of the ABC system used. (B) Lane 1, *P. syringae* S203 (the naturally occurring Ina$^+$ source organism of the *inaZ* gene); lane 2, *P. syringae* RGP36 (the Ina$^-$ deletion mutant of S203); lane 3, MS10 (*E. coli* carrying the *inaZ* gene); lane 4, CD3 [*E. coli* JC10291(pUC9), Ina$^-$ control]. Arrows mark bands at known migration positions of ice nucleation proteins. Lane B3 was loaded with 56 μg of protein; all other lanes were loaded with 28 μg of protein (about 10^8 CFU).

strain LC41 harbors a plasmid-borne clone of the *inaW* gene. Many faint bands of lower molecular size (M_r) were also visualized. Proteins derived from an isogenic Ina$^-$ *E. coli* strain, CD7 (Fig. 1A, lane 2), showed no reaction with anti-InaW. This demonstrated that anti-InaW reacted specifically with the ice nucleation protein. Thus, we concluded that the bands of lower M_r were related to the InaW protein.

The antibody concentration to be used was optimized by examining the intensity of staining produced by serial dilutions of the antiserum. Staining was observed at concentrations of antibody as low as 1:800 (based on serum concentration). However, an antibody dilution of 1:300 gave the best compromise between specificity and sensitivity. This antiserum dilution was used in all subsequent experiments.

Preparations from *P. fluorescens* MS1650 (Ina$^+$), *P. fluorescens* GJP17B (Ina$^-$), *P. syringae* S203 (Ina$^+$), and *P. syringae* RGP36 (Ina$^-$) were separated by SDS-PAGE and analyzed by Western blotting. The results of such analyses are also shown in Fig. 1. The Ina$^+$ organism (and source of the *inaW* gene) *P. fluorescens* MS1650 (Fig. 1A, lane 3) yielded samples which showed a strongly staining band migrating with the same M_r as InaW protein heterologously expressed by *E. coli* (Fig. 1A, lane 1). This band was absent in membranes derived from the isogenic Ina$^-$ strain *P. fluorescens* GJP17B (Fig. 1A, lane 4). A diffuse band of lower M_r was seen in both Ina$^+$ and Ina$^-$ strains. This band, which was visualized in the absence of primary antibody, was probably caused by cross-reacting secondary antibody (biotinylated goat anti-rabbit) or an avidin-binding protein (9).

Samples derived from the Ina$^+$ organism (and source of the *inaZ* gene) *P. syringae* S203 (Fig. 1B, lane 1) showed a band at the known migration position (32) of InaZ protein. A sample derived from *E. coli* strain MS10, which harbors a plasmid-borne clone of the *inaZ* gene, is shown for comparison in Fig. 1B, lane 3. Again, many discrete bands of lower M_r were observed. Samples derived from *P. syringae* RGP36, the Ina$^-$ deletion mutant of *P. syringae* S203 (Fig. 1B, lane 2), showed neither the parent band nor the lower-M_r bands. Finally, samples prepared from the Ina$^-$ *E. coli* strain CD3 (Fig. 1B, lane 4) showed no stained bands.

Treatment of membranes derived from *Pseudomonas* species with OSG prior to SDS-PAGE and Western blotting was absolutely required to obtain strongly immunostained nucleation protein bands. Western analyses of Ina$^+$ bacteria prepared for electrophoresis without an OSG wash showed faint ice nucleation protein bands when 1/10 of the total protein used for this study was analyzed. These bands faded and smeared as the protein level was increased until, at the levels reported here, they disappeared entirely (data not shown). Cross-reactive bands of lower M_r were also evident in these samples; the smaller of these did not fade as protein loading was increased. The source of the anomalous electrophoretic behavior of unwashed samples may have been the same as that observed for *Pseudomonas aeruginosa* membranes (8). It has been reported that treatment with the detergent lauryl sarcosyl removes approximately 70% of lipopolysaccharide from *P. aeruginosa* membranes and produces improvements in electrophoretic behavior similar to those we observed after OSG treatment (8).

Timing of expression of ice nucleation gene product and the Ina$^+$ phenotype. The timing of expression of the ice nucleation gene product and its correlation with the Ina$^+$ phenotype were examined for *P. syringae* S203 and *P. fluorescens* MS1650. Lawns of *P. syringae* S203 which had been inoculated simultaneously were sequentially harvested after 14, 18, 22, 37.5, 44, and 62.8 h of growth on NAG plates. At each harvest, an ice nucleation spectrum was determined. Another standard portion of cells was used to prepare a nucleating fraction, which was subsequently solubilized and prepared for SDS-PAGE and Western blotting. The results of the ice nucleation assays and Western analyses are shown in Fig. 2. The *P. syringae* S203 samples showed a marked increase in InaZ protein expression (Fig. 2A) and Ina$^+$

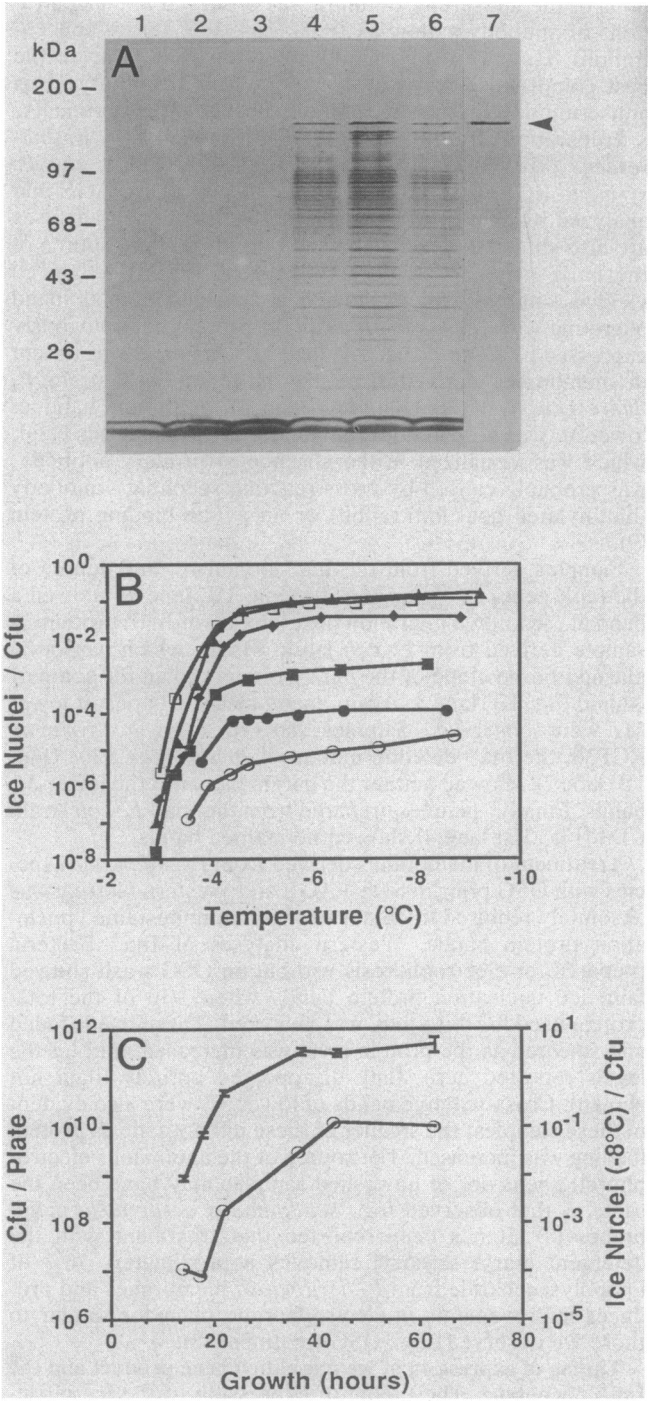

FIG. 2. Comparison of InaZ protein levels, Ina$^+$ phenotype, and growth phase in *P. syringae* S203. (A) Western analysis of proteins from *P. syringae* S203 plates harvested after 14, 18, 22, 37.5, 44, and 62.8 h of growth at 24°C (lanes 1 to 6, respectively); lane 7, 720 ng of InaZ protein (arrow) purified from MS10; other protein loadings were 28 μg per lane. (B) Ice nucleation spectra of cells from *P. syringae* S203 plates harvested after 14 (●), 18 (○), 22 (■), 37.5 (◆), 44 (□), and 62.8 (▲) h of growth at 24°C. (C) Comparison of a growth curve generated by serial dilution plating (error bars) and frequency of ice nuclei (per CFU) expressed at −8°C (○) at each harvest time point for *P. syringae* S203. Error bars are standard deviations for three to four determinations.

phenotype (Fig. 2B) over the time course. Ice nucleation activity increased from 1 nucleus per 10^5 cells to >1 nucleus per 10 cells. The relationship between culture growth and the frequency per cell of ice nuclei that were active at or above −8°C is shown in Fig. 2C; ice nuclei were not highly expressed until the culture reached the stationary phase. Growth of *P. syringae* S203 on minimal plates supplemented with the same glycerol concentration as in NAG led to final cell populations and final frequencies of nucleation per cell which were lower by a factor of 10; however, the data still indicated that the Ina$^+$ phenotype was not induced until the early stationary phase (data not shown).

The same procedure was followed with *P. fluorescens* MS1650 with different results, shown in Fig. 3. With this organism, detectable InaW protein (Fig. 3A) and ice nucleation activity (Fig. 3B) were nearly constant over the time course. Endogenous protease activity appeared to increase with time, so that InaW protein suffered considerably more degradation in the last three samples (lanes 4 to 6). Nucleation activity was approximately 1 nucleus per 100 cells. There was no significant correlation between ice nucleation frequency per cell and growth phase, as shown in Fig. 3C.

Identification of ice nucleation proteins in other species. It has been observed (20) that culture media and growth conditions strongly affect the ice nucleation activity of *P. syringae* PS31 and other Ina$^+$ bacteria. We used this information to find sets of conditions which yielded either high or low expression of ice nuclei in cultures of the naturally occurring ice-nucleating bacteria *P. syringae* PS31 and *E. herbicola* MS3000.

The Western analyses and ice nucleation spectra of *P. syringae* PS31 grown under different conditions are shown in Fig. 4A and C. When cells were grown on NAG plates at 24°C, they were similar in behavior to *P. syringae* S203. The Ina$^+$ phenotype was well expressed once the cells reached the stationary phase, and a high-M_r band with an associated family of bands of lower M_r was observed (Fig. 4A, lane 1). The parent band migrated with an M_r higher than that of the product of *inaZ* (Fig. 4A, lane 2). This agrees with the observation that the region of DNA encoding ice nucleation in *P. syringae* PS31 is longer than that encoding ice nucleation in *P. syringae* S203 (L. Corotto and G. Warren, personal communication). The same organism cultured in LB at 24°C showed greatly reduced ice nucleation activity (Fig. 4C) and no high-M_r protein detected by anti-InaW (Fig. 4A, lane 3).

Similar results were obtained when cultures of *E. herbicola* MS3000 grown on NAG plates were compared with cultures grown in LB. Figures 4B and C show the Western analyses and ice nucleation spectra for this organism under various culture conditions. *Erwinia herbicola* grown on NAG for 18 h at 24°C and then for 48 h at 8°C (Fig. 4B, lane 2) or 24°C (lane 5) showed relatively high ice nucleation activity. In both experiments, a set of high-M_r bands was observed. This group of bands was absent in Fig. 4B, lane 3, which was derived from cells grown in LB for 48 h at room temperature. Under these conditions, the Ina$^+$ phenotype was also greatly depressed (Fig. 4C). *Erwinia carotovora* Ecc301 was included in Fig. 4B, lane 4, as a nonnucleating member of the genus *Erwinia*. When grown under the conditions which yielded high nucleation activity for *P. syringae* PS31 and moderate activity for *E. herbicola* MS3000, *E. carotovora* yielded no measurable ice nucleation activity, and no high-M_r protein was detected by anti-InaW.

Periodic degradation of the InaZ protein. To determine whether the periodic bands observed in Fig. 2 were due to

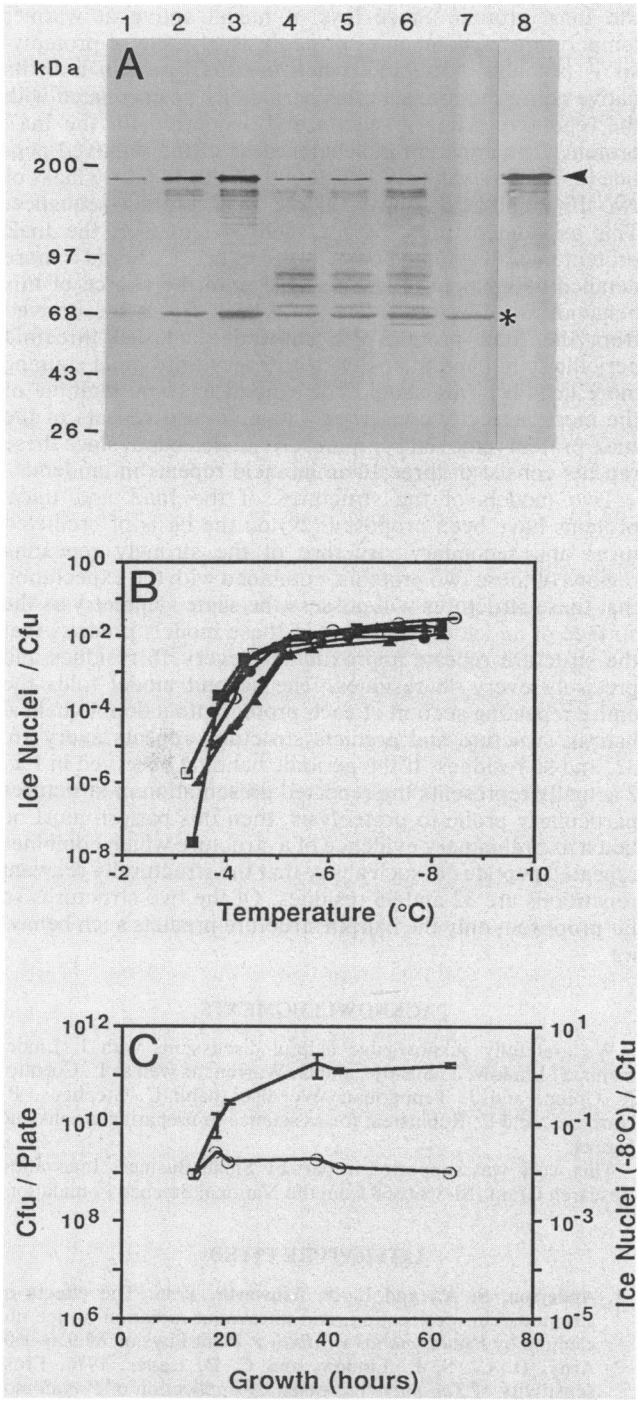

FIG. 3. Comparison of InaW protein levels, Ina$^+$ phenotype, and growth phase in *P. fluorescens* MS1650. (A) Western analysis of proteins from *P. fluorescens* MS1650 plates harvested after 14.3, 18.5, 21, 38, 42.8, and 64 h of growth at 24°C (lanes 1 to 6, respectively). Protein loadings were 28 μg per lane. Lane 7 is derived from *P. fluorescens* GJP17B (* marks the avidin-binding band) and lane 8 from LC41 (arrow marks the InaW protein). (B) Ice nucleation spectra of cells from *P. fluorescens* MS1650 plates harvested after 14.25 (●), 18.5 (○), 21 (■), 38 (◆), 42.75 (□), and 64 (▲) h of growth at 24°C. (C) Comparison of a growth curve generated by serial dilution plating (error bars) and frequency of ice nuclei (per CFU) expressed at −8°C (○) at each harvest time point for *P. fluorescens* MS1650. Error bars, Same as in Fig. 2 legend.

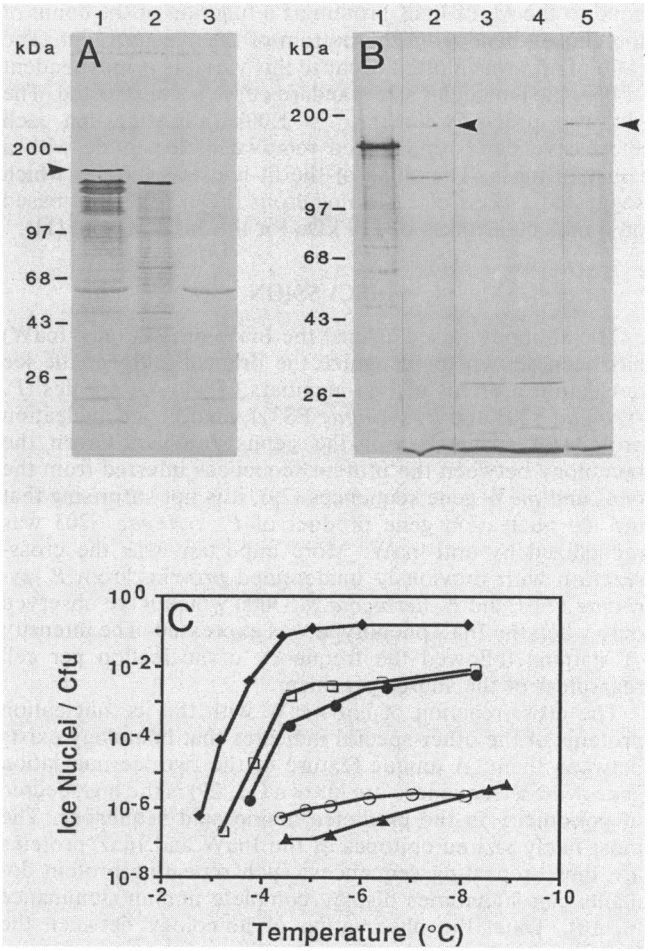

FIG. 4. Presence or absence of high-M_r proteins detected by Western analysis, and corresponding presence or absence of the Ina$^+$ phenotype. Bacterial protein loadings were 28 μg per lane. (A) Lane 1, proteins from *P. syringae* PS31 grown on NAG plates for 48 h at 24°C; lane 2, InaZ protein (720 ng); lane 3, *P. syringae* PS31 grown in LB. (B) Lane 1, InaZ protein (720 ng); lane 2, *E. herbicola* MS3000 grown on NAG plates for 18 h at 24°C and then for 48 h at 8°C; lane 3, *E. herbicola* MS3000 grown for 48 h in LB; lane 4, *E. carotovora* Ecc301 grown for 18 h at 24°C and then for 48 h at 8°C; lane 5, *E. herbicola* MS3000 grown for 48 h at 24°C. Arrows mark the positions of the largest proteins which appeared with the Ina$^+$ phenotype. (C) Ice nucleation spectra of *P. syringae* PS31 grown on NAG plates for 48 h at 24°C (◆), *E. herbicola* MS3000 grown on NAG plates for 18 h at 24°C and then for 48 h at 8°C (□), *E. herbicola* MS3000 grown on NAG plates for 48 h at 24°C (●), and *E. herbicola* MS3000 (○) and *P. syringae* PS31 (▲) grown in LB for 48 h.

proteolytic degradation of the InaZ protein, nuclei prepared from stationary-phase *P. syringae* S203 were aged for various periods of time at room temperature and then analyzed by Western blotting. There was a striking increase in the intensity of staining of cross-reactive bands of lower M_r with increasing sample age; the intensity of the parent InaZ protein band decreased as the intensities of the lower bands increased (data not shown). These data indicate that some agent, possibly a protease, degraded the InaZ protein. Prolonged incubation at room temperature also produced a 100-fold decrease in nuclei functioning at or above −6°C, but did not much affect nuclei functioning at or below −8°C.

The pattern of cross-reactive bands (Fig. 2A) was interpreted by plotting the ratio of the M_r of a given proteolytic

band to the M_r of InaZ protein as a function of the count of the chosen band from the bottom of the Western blot. The ratio of M_rs was plotted because this variable is independent of how the molecular size standard curve is constructed. The plot was precisely linear ($r^2 = 1.00$), indicating that each successive band represented removal of a peptide with a constant mass. The slope of the fit line was 0.0219, which suggested a mass of 2.61 kilodaltons (kDa) per band, based on a molecular mass of 119 kDa for the InaZ protein (11).

DISCUSSION

The antibody raised against the InaW protein (anti-InaW) has been shown to recognize the original antigen, the ice nucleation proteins of two members of another species (*P. syringae* S203 and *P. syringae* PS31), and the ice nucleation protein of a member of the genus *Erwinia*. Given the homology between the protein sequences inferred from the *inaZ* and *inaW* gene sequences (29), it is not surprising that the ice nucleation gene product of *P. syringae* S203 was recognized by anti-InaW. More important was the cross-reaction with previously unidentified proteins from *P. syringae* PS31 and *E. herbicola* MS3000 which were observed only when the Ina$^+$ phenotype was expressed. The intensity of staining followed the frequency of nucleation per cell regardless of the source organism.

The cross-reaction of anti-InaW with the ice nucleation proteins of the other species indicates that homology exists between them. A unique feature of the two ice nucleation genes whose sequences are known (11, 29) is the high degree of periodicity in the predicted amino acid sequences. The most likely shared epitopes of the InaW and InaZ proteins are these repeating sequences; such repeating protein domains can sometimes display complete immunodominance (6, 10). Thus, the observation of homology between the InaW protein and the two new ice nucleation proteins identified may indicate that these two proteins contain the same repeated sequences.

The conditions necessary to achieve optimal expression of ice nuclei varied among organisms. With the organisms *P. syringae* S203 and *P. syringae* PS31, high Ina$^+$ expression did not occur until cells reached the stationary phase. Clearly, in these two bacterial strains, the transition to stationary phase is accompanied by a signal which induces expression of the Ina$^+$ phenotype. Ice nucleation activity and ice nucleation protein appeared to be constitutively expressed in the organism *P. fluorescens* MS1650, as shown in Fig. 3C. However, at both high and low temperatures, the numbers of active nuclei were at least a factor of 10 lower than in stationary-phase *P. syringae* S203. The differences observed between *P. syringae* and *P. fluorescens* may reflect different strategies of ice nucleus expression. What might be the nature of the signal which turns on the Ina$^+$ phenotype in *P. syringae*? Probable signal mechanisms are metabolite accumulation or nutrient depletion. Either signal would be consistent with the observed loss of nucleation activity in *P. syringae* PS31 during submerged growth: nutrient and metabolite gradients arise in the unstirred plate environment which are dispersed in liquid culture.

The results of the Western analysis of the degradation time course experiment demonstrate that the cross-reacting bands of lower M_r apparent on many of our Western blots were derived from ice nucleation proteins by some sort of proteolytic degradation. The loss of warm-threshold nuclei observed in the aged samples could be an effect of this proteolysis. The observed pattern of proteolytic fragments implies that a preferred site of proteolysis occurs regularly in the InaZ protein. Since loss of nuclei active at warmer temperatures accompanies proteolysis, the site of proteolysis is probably accessible when the InaZ protein is in its native conformation. Can this periodicity be correlated with the repetitive primary sequence (11) inferred for the InaZ protein? The apparent molecular mass of the removed peptide (2.61 kDa) was only 15% less than the 3.06-kDa mass of two 16-amino-acid repeats in the InaZ protein sequence. This assignment must be regarded as tentative; the InaZ protein migrates anomalously on SDS gels (32), and a more detailed assignment is not possible until the source of this behavior is understood. The pattern of fragments derived from the InaZ protein also showed a marked threefold periodicity in band intensity, with every third band staining more heavily. This should correspond to some multiple of the more perfectly conserved 48-amino-acid repeats of the InaZ protein removed per intensely stained band, since these repeats consist of three 16-amino-acid repeats in tandem.

Two models of the structures of the InaZ and InaW proteins have been proposed (29) on the basis of predicted turns and secondary structure of the strongly repeating regions of these two proteins, combined with the expectation that these structures will possess the same symmetry as the surface of an ice crystal. One of these models predicts that the structure repeats approximately every 16 residues and precisely every 48 residues. The second model folds the entire repeating section of each protein into a double-helical hairpin structure and predicts structural repeats every 16, 32, and 96 residues. If the periodic banding observed in Fig. 2 actually represents the repeated presentation of structures particularly prone to proteolysis, then this pattern must be taken as preliminary evidence of a structure which combines repeated peptides in such a way that the structurally relevant repetitions are 32 and 96 residues. Of the two structures so far proposed, only the hairpin structure predicts such behavior.

ACKNOWLEDGMENTS

We gratefully acknowledge helpful discussions with J. Lindemann, S. Lindow, T. Suslow, and G. Warren, as well as L. Corotto, R. Green, and J. Tepperman. We also thank C. Stephens, R. Narberes, and C. Rubinstein for assistance in preparing graphs and figures.

This work was supported in part by Small Business Innovation Research Grant ISI-8660868 from the National Science Foundation.

LITERATURE CITED

1. **Anderson, S. A., and E. N. Ashworth.** 1986. The effects of streptomycin, desiccation, and ultraviolet radiation on ice nucleation by *Pseudomonas viridiflava*. Plant Physiol. **80**:956–960.
2. **Arny, D. C., S. E. Lindow, and C. D. Upper.** 1976. Frost sensitivity of *Zeo mays* increased by application of *Pseudomonas syringae*. Nature (London) **262**:282–284.
3. **Caple, G., D. C. Sands, R. G. Layton, W. V. Zucker, and J. R. Snider.** 1986. Biogenic ice nucleation: could it be metabolically initiated? J. Theor. Biol. **119**:37–45.
4. **Chang, A. C. Y., and S. N. Cohen.** 1978. Construction and characterization of amplifiable multicopy DNA cloning vehicles derived from the P15A cryptic miniplasmid. J. Bacteriol. **134**: 1141–1156.
5. **Corotto, L. V., P. K. Wolber, and G. J. Warren.** 1986. Ice nucleation activity of *Pseudomonas fluorescens*: mutagenesis, complementation analysis, and identification of a gene product. EMBO J. **5**:231–236.
6. **Dame, J. B., J. L. Williams, T. F. McCutchan, J. L. Weber, R. A. Wirtz, W. T. Hockmeyer, W. L. Maloy, J. D. Haynes, I.**

Schneider, D. Roberts, G. S. Sanders, E. P. Reddy, C. L. Diggs, and L. H. Miller. 1984. Structure of the gene encoding the immunodominant surface antigen on the sporozoite of the human malaria parasite *Plasmodium falciparum*. Science **225:** 593–599.

7. **Dandliker, W. B., M. Hsu, J. Levin, and B. R. Rao.** 1981. Equilibrium and kinetic inhibition assays based upon fluorescence polarization. Methods Enzymol. **74:**3–28.
8. **DeWeger, L. A., R. van Boxtel, B. van der Burg, R. Grutters, F. P. Geels, B. Schippers, and B. Lugtenberg.** 1986. Siderophores and outer membrane proteins of antagonistic, plant-growth-stimulating, root-colonizing *Pseudomonas* spp. J. Bacteriol. **165:**585–594.
9. **Gardner, L.** 1983. Non-radioactive DNA labelling: detection of specific DNA and RNA sequences on nitrocellulose and *in situ* hybridizations. Biotechniques **1:**38–40.
10. **Godson, G. N., J. Ellis, P. Svec, D. H. Schlesinger, and V. Nussenzweig.** 1983. Identification and chemical synthesis of a tandemly repeated immunogenic region of *Plasmodium knowlesi* circumsporozoite protein. Nature (London) **305:**29–33.
11. **Green, R. L., and G. J. Warren.** 1985. Physical and functional repetition in a bacterial ice nucleation gene. Nature (London) **317:**645–648.
12. **Hunkapiller, M. W., E. Lujan, F. Ostrander, and L. Hood.** 1983. Isolation of microgram quantities of protein from polyacrylamide gels for amino acid sequence analysis. Methods Enzymol. **91:**227–236.
13. **Ito, K., T. Sato, and T. Yura.** 1977. Synthesis and assembly of the membrane proteins in *E. coli*. Cell **11:**551–559.
14. **Kozloff, L. M., M. Lute, and D. Westaway.** 1984. Phosphatidylinositol as a component of the ice nucleating site of *Pseudomonas syringae* and *Erwinia herbicola*. Science **226:**845–846.
15. **Laemmli, U. K.** 1970. Cleavage of structural proteins during the assembly of the head of bacteriophage T4. Nature (London) **227:**680–685.
16. **Lindow, S. E.** 1982. Epiphytic ice nucleation-active bacteria, p. 335–362. *In* M. S. Mount and G. H. Lacy (ed.), Phytopathogenic prokaryotes. Academic Press, Inc., New York.
17. **Lindow, S. E.** 1983. The role of bacterial ice nucleation in frost injury to plants. Annu. Rev. Phytopathol. **21:**363–384.
18. **Lindow, S. E.** 1983. Methods of preventing frost injury caused by epiphytic ice-nucleation-active bacteria. Plant Dis. **67:**327–333.
19. **Lindow, S. E., D. C. Arny, and C. D. Upper.** 1978. *Erwinia herbicola*: a bacterial ice nucleus active in increasing frost injury to corn. Phytopathology **68:**523–527.
20. **Lindow, S. E., S. S. Hirano, W. R. Barchet, D. C. Arny, and C. D. Upper.** 1982. Relationship between ice nucleation frequency of bacteria and frost injury. Plant Physiol. **70:**1090–1093.
21. **Maki, L. R., E. L. Galyan, M. M. Chang-Chien, and D. R. Caldwell.** 1974. Ice nucleation induced by *Pseudomonas syringae*. Appl. Microbiol. **28:**456–459.
22. **Maki, L. R., and K. J. Willoughby.** 1978. Bacteria as biogenic sources of freezing nuclei. J. Appl. Meteorol. **17:**1049–1053.
23. **Orser, C., B. J. Staskawicz, N. J. Panopoulos, D. Dahlbeck, and S. E. Lindow.** 1985. Cloning and expression of bacterial ice nucleation genes in *Escherichia coli*. J. Bacteriol. **164:**359–366.
24. **Phelps, P., T. H. Giddings, M. Prochoda, and R. Fall.** 1986. Release of cell-free ice nuclei by *Erwinia herbicola*. J. Bacteriol. **167:**496–502.
25. **Smith, P. K., R. I. Krohn, G. T. Hermanson, A. K. Mallia, F. H. Gartner, M. D. Provenzano, E. K. Fujimoto, N. M. Goeke, B. J. Olson, and D. C. Klenk.** 1985. Measurement of protein using bicinchoninic acid. Anal. Biochem. **150:**76–85.
26. **Towbin, H., T. Staehelin, and J. Gordon.** 1979. Electrophoretic transfer of proteins from polyacrylamide gels to nitrocellulose sheets: procedure and some applications. Proc. Natl. Acad. Sci. USA **76:**4350–4354.
27. **Vali, G.** 1971. Quantitative evaluation of experimental results on the heterogeneous freezing nucleation of supercooled liquids. J. Atmos. Sci. **28:**402–409.
28. **Vieira, J., and J. Messing.** 1982. The pUC plasmids, an M13mp7-derived system for insertional mutagenesis and sequencing with synthetic universal primers. Gene **19:**259–268.
29. **Warren, G., L. Corotto, and P. K. Wolber.** 1986. Conserved repeats in diverged ice nucleation structural genes from two species of *Pseudomonas*. Nucleic Acids Res. **14:**8047–8068.
30. **Warren, G. J., J. Lindemann, T. V. Suslow, and R. L. Green.** 1987. Ice nucleation deficient bacteria as frost protection agents, p. 215–227. *In* H. M. LeBaron, R. O. Mumma, R. C. Honeycutt, and J. H. Duesing (ed.), ACS Symposium Series No. 334: Biotechnology in agricultural chemistry. American Chemical Society Books, Washington, D.C.
31. **Willis, D. K., B. E. Uhlin, K. S. Amini, and A. J. Clark.** 1981. Physical mapping of the *srl recA* region of *Escherichia coli*: analysis of Tn*10* generated insertions and deletions. Mol. Gen. Genet. **183:**497–504.
32. **Wolber, P. K., C. A. Deininger, M. W. Southworth, J. Vandekerckhove, M. van Montagu, and G. J. Warren.** 1986. Identification and purification of a bacterial ice nucleation protein. Proc. Natl. Acad. Sci. USA **83:**7256–7260.
33. **Young, R. A., and R. W. Davis.** 1983. Efficient isolation of genes by using antibody probes. Proc. Natl. Acad. Sci. USA **80:**1194–1198.